ACS APPLIED MATERIALS & INTERFACES

Research Article

www.acsami.org

Improvement of the Cycling Performance of $LiNi_{0.6}Co_{0.2}Mn_{0.2}O_2$ Cathode Active Materials by a Dual-Conductive Polymer Coating

Seo Hee Ju,[†] Ik-Su Kang,[‡] Yoon-Sung Lee,[‡] Won-Kyung Shin,[‡] Saheum Kim,[§] Kyomin Shin,[§] and Dong-Won Kim*[,‡]

[†]Battery Materials R&D Center, GS Energy, Seoul 134-848, Korea

[‡]Department of Chemical Engineering, Hanyang University, Seoul 133-791, Korea

[§]R&D Division, Hyundai Motor Company, Hwaseong-si, Gyeonggi-do 445-706, Korea

Supporting Information

ABSTRACT: $LiNi_{0.6}Co_{0.2}Mn_{0.2}O_2$ cathode materials were surface-modified by coating with a dual conductive poly(3,4-ethylenedioxythiophene)-*co*-poly(ethylene glycol) (PEDOT-*co*-PEG) copolymer, and their resulting electrochemical properties were investigated. The surface-modified $LiNi_{0.6}Co_{0.2}Mn_{0.2}O_2$ cathode material exhibited a high discharge capacity and good high rate performance due to enhanced transport of Li^+ ions as well as electrons. The presence of a protective conducting polymer layer formed on the cathode also suppressed the growth of a resistive layer and inhibited the dissolution of transition metals from the active cathode materials, which resulted in more stable cycling characteristics than the pristine $LiNi_{0.6}Co_{0.2}Mn_{0.2}O_2$ cathode material at 55 °C.

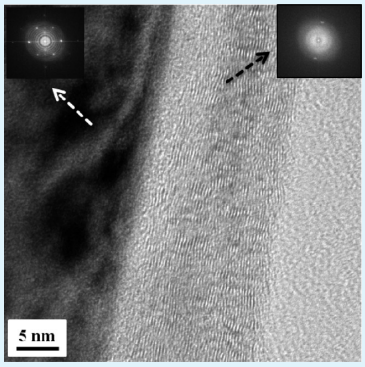

KEYWORDS: *conductive polymer, surface modification, $LiNi_{0.6}Co_{0.2}Mn_{0.2}O_2$, protective coating, cycling performance*

INTRODUCTION

Rechargeable lithium-ion batteries have become the main power sources for portable electronic devices due to their high energy density and long cycle life and are actively being developed as power supplies for electric vehicles and energy storage systems.[1,2] As an active cathode material, $LiCoO_2$ has been widely used in commercialized lithium-ion batteries due to its good cycling performance, low irreversible capacity loss, and ease of synthesis. However, the high cost and toxicity of cobalt pose major obstacles that limit its application in large capacity lithium-ion batteries such as electric vehicles. As a result, layered $LiNi_xCo_yMn_{1-x-y}O_2$ materials have attracted much attention as promising alternative cathode materials because of their high capacity, relatively low cost, good cycling stability, and improved safety.[3−11] However, the materials become unstable if they are charged above 4.2 V at elevated temperatures due to the dissolution of transition metals from the host structure and decomposition of the organic electrolyte at high voltage. To solve these problems, extensive studies have been carried out to coat the surface of cathode active materials with conductive polymers as well as inorganic materials.[12−29] The surface modification of cathode materials with a conductive polymer is quite beneficial with respect to the delivery of the original capacity without a reduction of the amount of the electrochemically active element in the parent cathode materials. Among various conductive polymers, poly(3,4-ethylenedioxythiophene) (PEDOT) is one of the promising coating materials due to its high electronic conductivity and good electrochemical stability.[29−35] However, PEDOT is not an ionic conductive polymer but an electronic conductive polymer. In order to enhance the charge transfer reaction on the electrode surface, it is highly desirable to use dual-conductive polymers that transport both electrons and Li^+ ions through the surface layer. In our previous study, a thin polymer layer based on poly(3,4-ethylenedioxythiophene)-*co*-poly(ethylene glycol) (PEDOT-*co*-PEG) block copolymer was coated onto lithium electrode to suppress the electrolyte decomposition and dendrite growth during cycling.[36] In the copolymer, PEG is a highly ion-conductive polymer that transports lithium ions. The biconductive polymer coating on the lithium metal caused the capacity retention of the Li/$LiCoO_2$ cell to increase from 9.3% to 87.3% after 200 cycles compared to the cell with the pristine lithium electrode. These results prompted us to use PEDOT-*co*-PEG block copolymer as a conductive coating material on $LiNi_xCo_yMn_{1-x-y}O_2$ cathode materials. Fedorkova et al. also reported that surface modification of $LiFePO_4$ cathode particles by blending polypyrrole with PEG is an attractive route to improve their mechanical properties and electrical conductivity.[26,27] However, to the best of our knowledge, there are no published reports of a copolymer coated on cathode active materials exhibiting mixed electronic-ionic conductivity resulting in improved

Received: November 6, 2013
Accepted: January 24, 2014
Published: January 24, 2014

   dx.doi.org/10.1021/am404965p | ACS Appl. Mater. Interfaces 2014, 6, 2546−2552

electrochemical properties. In this work, we synthesized $LiNi_{0.6}Co_{0.2}Mn_{0.2}O_2$ cathode materials with high discharge capacity. Their surface was modified by coating with dual-conductive PEDOT-*co*-PEG copolymer in order to improve their electrochemical performance. The surface modification of the $LiNi_{0.6}Co_{0.2}Mn_{0.2}O_2$ cathode materials with the PEDOT-*co*-PEG copolymer was demonstrated to be very effective in improving their cycling stability and high rate performance.

EXPERIMENTAL SECTION

Surface Modification of $LiNi_{0.6}Co_{0.2}Mn_{0.2}O_2$ Particles. The $LiNi_{0.6}Co_{0.2}Mn_{0.2}O_2$ materials were synthesized as described in the Supporting Information.[16] PEDOT or PEDOT-*co*-PEG solution (Aldrich) was dispersed in N-methyl pyrrolidone (NMP) at a concentration of 10 wt %. The $LiNi_{0.6}Co_{0.2}Mn_{0.2}O_2$ powders were immersed in the polymer solution, and the mixture was stirred at 60 °C for 4 h to induce surface coating of the $LiNi_{0.6}Co_{0.2}Mn_{0.2}O_2$ powders. After filtering the mixed solution and drying under vacuum at 110 °C for 24 h, the surface-modified $LiNi_{0.6}Co_{0.2}Mn_{0.2}O_2$ powders were finally obtained.

Electrode Preparation and Cell Assembly. The positive electrode was prepared by coating the NMP-based slurry containing surface-modified $LiNi_{0.6}Co_{0.2}Mn_{0.2}O_2$ powders, poly(vinylidene fluoride) (PVdF), and super-P carbon (MMM co.) (85:7.5:7.5 by weight) on aluminum foil. After drying under vacuum at 120 °C overnight, the electrode was punched into a disk. The geometrical area of the positive electrode was 1.54 cm^2, and its active mass loading corresponded to a capacity of about 1.0 mAh cm^{-2}. The lithium electrode consisted of a 100 μm thick lithium foil that was pressed onto a copper current collector. A CR2032-type coin cell composed of a lithium negative electrode, a polypropylene separator (Celgard 2400), and a $LiNi_{0.6}Co_{0.2}Mn_{0.2}O_2$ positive electrode was assembled with a liquid electrolyte. The liquid electrolyte used was 1 M $LiPF_6$ in ethylene carbonate (EC)/dimethyl carbonate (DMC) (1:1 by volume, battery grade, Soulbrain Co. Ltd.). All cells were assembled in a drybox filled with argon gas.

Characterization and Measurements. The elemental analysis of PEDOT-*co*-PEG copolymer was carried out on an elemental analyzer (Flash EA 1112series, CE Instruments) in order to estimate the relative molar ratio of PEDOT and PEG. The electronic conductivities of the pressed $LiNi_{0.6}Co_{0.2}Mn_{0.2}O_2$ powders before and after polymer coating were measured by a four point probe method with a surface resistivity measurement system (CMT-SR1000N, Changmin Tech.) in which disk samples were contacted with a four-point probe at room temperature. In order to measure to ionic conductivity, the PEDOT-*co*-PEG film was soaked with liquid electrolyte (1 M $LiPF_6$ in EC/DMC) and sandwiched between two stainless steel electrodes. AC impedance measurement was then performed to measure ionic conductivity using an impedance analyzer over the frequency range of 100 Hz to 100 kHz. Fourier transform infrared (FTIR) spectra were recorded on JASCO 460 IR spectrometer using KBr pellets in the range of 400-4000 cm^{-1}. Powder X-ray diffraction (XRD) (Rigaku, Rint-2000) using Cu Kα radiation was used to identify the crystalline phase of the pristine and surface-modified $LiNi_{0.6}Co_{0.2}Mn_{0.2}O_2$ powders. Thermogravimetric analysis (TGA) was conducted on simultaneous TGA/DSC analyzer (SDT Q600, TA Instrument) at a heating rate of 5 °C min^{-1} under N_2 flow. The elemental distribution on the surface of the modified $LiNi_{0.6}Co_{0.2}Mn_{0.2}O_2$ particles was examined using energy dispersive X-ray spectroscopy (EDX). The surface morphologies of the $LiNi_{0.6}Co_{0.2}Mn_{0.2}O_2$ powders before and after polymer coating were observed using field emission transmission electron microscopy (FE-TEM, Tecnai G2 F30). Charge and discharge cycling tests of the $Li/LiNi_{0.6}Co_{0.2}Mn_{0.2}O_2$ cells were conducted at different current densities over the voltage range of 2.8–4.3 V using battery testing equipment (WBCS 3000, Wonatech). AC impedance measurements of the $Li/LiNi_{0.6}Co_{0.2}Mn_{0.2}O_2$ cells were performed in the charged state using a Zahner Electrik IM6 impedance analyzer over the frequency range of 1 mHz to 100 kHz with an amplitude of 10 mV. For the quantitative measurement of transition metal ion dissolution, the fully charged cells were carefully disassembled to obtain the charged $LiNi_{0.6}Co_{0.2}Mn_{0.2}O_2$ electrodes. These electrodes were stored in fresh liquid electrolyte at 55 °C. The metal content dissolved in the liquid electrolyte was then measured as a function of storage time using an atomic absorption spectroscopy (AA, vario 6, Analyticjena).

RESULTS AND DISCUSSION

The morphologies of the $LiNi_{0.6}Co_{0.2}Mn_{0.2}O_2$ particles were characterized by uniform and large spherical agglomerates (8–10 μm) composed of small primary particles (see Figure S1 in the Supporting Information). The rock-shaped primary particles slightly protrude towards the outside of the secondary structure of the particles. Figure 1 presents the SEM image and

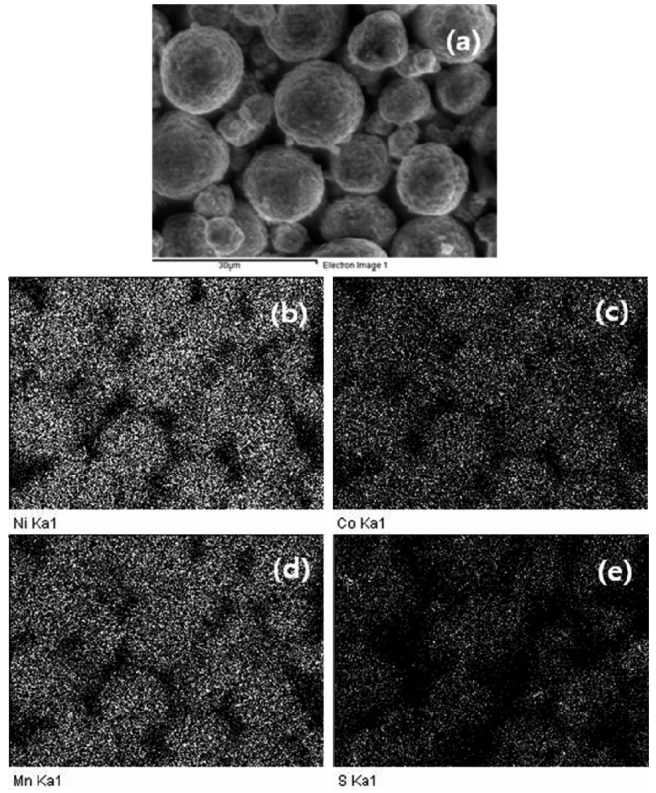

Figure 1. (a) SEM image of the surface-modified $LiNi_{0.6}Co_{0.2}Mn_{0.2}O_2$ particles and EDX mapping images of (b) Ni, (c) Co, (d) Mn, and (e) sulfur in the surface-modified $LiNi_{0.6}Co_{0.2}Mn_{0.2}O_2$ particles.

EDX mapping images of Ni, Co, Mn, and sulfur in the $LiNi_{0.6}Co_{0.2}Mn_{0.2}O_2$ particles coated by the PEDOT-*co*-PEG copolymer. Homogeneous distributions of Ni, Mn, and Co were observed in the $LiNi_{0.6}Co_{0.2}Mn_{0.2}O_2$ active material. It is also seen that the sulfur elements arising from the PEDOT-*co*-PEG copolymer are evenly distributed across the image (Figure 1e), which indicates that the surface of the $LiNi_{0.6}Co_{0.2}Mn_{0.2}O_2$ active material is uniformly coated with the PEDOT-*co*-PEG copolymer. The weight percentage of the PEDOT-*co*-PEG copolymer coated on the $LiNi_{0.6}Co_{0.2}Mn_{0.2}O_2$ particle was determined to be about 0.78% by a thermogravimetric analysis. The molar ratio of PEDOT and PEG in the copolymer was determined to be about 41:59 by elemental analysis.

Figure 2 shows the high resolution TEM images of the $LiNi_{0.6}Co_{0.2}Mn_{0.2}O_2$ particles before and after surface coating by the PEDOT-*co*-PEG copolymer. The pristine Li-

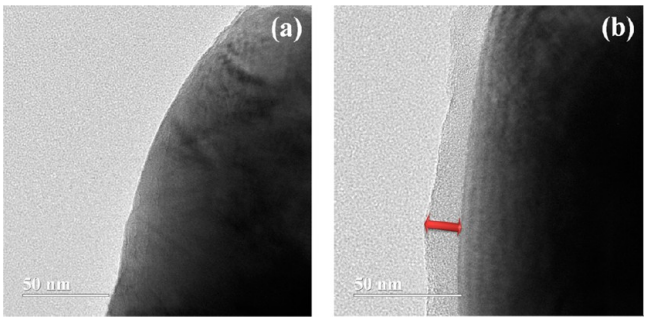

Figure 2. TEM images of (a) pristine $LiNi_{0.6}Co_{0.2}Mn_{0.2}O_2$ and (b) surface-modified $LiNi_{0.6}Co_{0.2}Mn_{0.2}O_2$ particles.

$Ni_{0.6}Co_{0.2}Mn_{0.2}O_2$ particle does not have an extra film on the particle surface, as shown in Figure 2a. On the contrary, the magnified image around the edge of the surface-modified $LiNi_{0.6}Co_{0.2}Mn_{0.2}O_2$ particle shown in Figure 2b reveals that it is uniformly coated by a thin conductive polymer layer which has a thickness ranging from 11 to 18 nm. As compared to conventional metal-oxide coating yielding discontinuous deposition of electrically inert layer, the distinctive features of the PEDOT-*co*-PEG layer are the highly continuous surface coverage with high electronic and ionic conductivity. The thin PEDOT-*co*-PEG layer on the $LiNi_{0.6}Co_{0.2}Mn_{0.2}O_2$ particle hardly affected the packing density of the electrode. The electronic conductivity of surface-modified $LiNi_{0.6}Co_{0.2}Mn_{0.2}O_2$ particles was measured to be 0.2 S cm^{-1}, which was much higher than that of pristine $LiNi_{0.6}Co_{0.2}Mn_{0.2}O_2$ particles (1.6×10^{-6} S cm^{-1}). The ionic conductivity of the PEDOT-*co*-PEG film soaked with the liquid electrolyte (1 M $LiPF_6$ in EC/DMC) was 4.2×10^{-3} S cm^{-1}, indicating fast ion transport through the thin surface layer.

The selected area electron diffraction (SAED) patterns obtained from the $LiNi_{0.6}Co_{0.2}Mn_{0.2}O_2$ particle and the PEDOT-*co*-PEG layer of the surface-modified $LiNi_{0.6}Co_{0.2}Mn_{0.2}O_2$ particle are shown in the left and right insets of Figure 3, respectively. The SAED pattern corresponding to the $LiNi_{0.6}Co_{0.2}Mn_{0.2}O_2$ particle (left side) exhibits some bright spot patterns, which is typical for crystalline $LiNi_{0.6}Co_{0.2}Mn_{0.2}O_2$ materials. On the other hand, the image in the right inset shows a hollow ring pattern without bright spots, indicating that the coating layer consisted of disordered polymer materials. Thus, these results provide conclusive evidence that the primary $LiNi_{0.6}Co_{0.2}Mn_{0.2}O_2$ particles are uniformly coated by the thin conductive polymer layer.

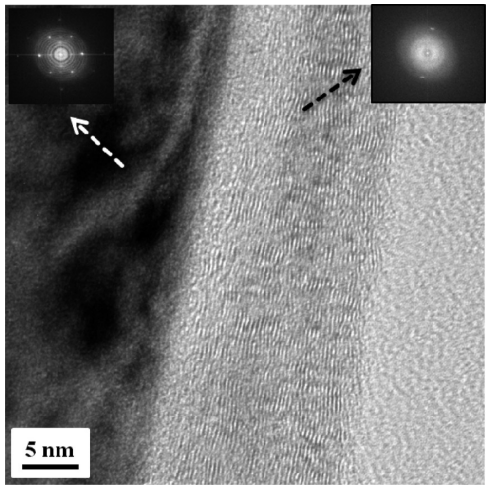

Figure 3. TEM image and SAED patterns of the surface-modified $LiNi_{0.6}Co_{0.2}Mn_{0.2}O_2$ particle (left SAED: $LiNi_{0.6}Co_{0.2}Mn_{0.2}O_2$ particle, right SAED: coating layer).

The existence of PEDOT-*co*-PEG on the $LiNi_{0.6}Co_{0.2}Mn_{0.2}O_2$ particle was further confirmed by comparison of the FTIR spectra of pristine and surface-modified $LiNi_{0.6}Co_{0.2}Mn_{0.2}O_2$ particles. As shown in Figure S2, the pristine $LiNi_{0.6}Co_{0.2}Mn_{0.2}O_2$ particle exhibits a broad band around 540 cm^{-1}, which comes from the M−O vibration.[37,38] No significant shift could be observed after polymer coating in this region, indicating no strong interactions between PEDOT-*co*-PEG and $LiNi_{0.6}Co_{0.2}Mn_{0.2}O_2$. The presence of PEDOT-*co*-PEG could be confirmed by the C═C ring and C−O−R vibration in PEDOT at about 1120 cm^{-1} and C−O−C stretching vibration in PEG at 1057 cm^{-1}.[29,39] XRD patterns for the pristine and surface-modified $LiNi_{0.6}Co_{0.2}Mn_{0.2}O_2$ powders are compared in Figure S3. All of the diffraction patterns were indexed to a hexagonal a-$NaFeO_2$ structure with an *R3m* space group without any impurity phases. Both of the 006/112 and 108/110 double peaks were split, which indicates that powders with a hexagonal layered structure were formed.[16] No significant differences in the XRD patterns between the pristine $LiNi_{0.6}Co_{0.2}Mn_{0.2}O_2$ and surface-modified $LiNi_{0.6}Co_{0.2}Mn_{0.2}O_2$ powders were observed. This result demonstrates that the surface modification of the $LiNi_{0.6}Co_{0.2}Mn_{0.2}O_2$ powders using the PEDOT-*co*-PEG copolymer has no influence on the crystal structure of the host materials.

Cycling performances of the Li/$LiNi_{0.6}Co_{0.2}Mn_{0.2}O_2$ cells with pristine and surface-modified active cathode materials were evaluated. Figure 4a presents the initial charge and discharge curves of the cells with pristine and surface-modified $LiNi_{0.6}Co_{0.2}Mn_{0.2}O_2$ particles in the voltage range of 2.8 to 4.3 V at a constant current rate of 0.1 C. The $LiNi_{0.6}Co_{0.2}Mn_{0.2}O_2$ cathode material coated by PEDOT-*co*-PEG delivered a slightly higher discharge capacity (184.3 $mAhg^{-1}$) than the pristine $LiNi_{0.6}Co_{0.2}Mn_{0.2}O_2$ cathode material (181.5 $mAhg^{-1}$). The conductive polymer coating is expected to reduce the contact resistance between the active cathode particles and facilitate electron transport in the positive electrode. It is also plausible that the PEDOT-*co*-PEG layer can provide reversible capacity as a cathode active material. As a result, the $LiNi_{0.6}Co_{0.2}Mn_{0.2}O_2$ cathode material coated by the PEDOT-*co*-PEG copolymer exhibited a higher discharge capacity. After two cycles at 0.1 C rate, cycling tests of Li/$LiNi_{0.6}Co_{0.2}Mn_{0.2}O_2$ cells with pristine and modified $LiNi_{0.6}Co_{0.2}Mn_{0.2}O_2$ were performed at a constant current rate of 90 mA g^{-1} (0.5 C rate), and the results are compared in Figure 4b. The initial discharge capacity of the surface-modified $LiNi_{0.6}Co_{0.2}Mn_{0.2}O_2$ materials is slightly higher than that of the pristine $LiNi_{0.6}Co_{0.2}Mn_{0.2}O_2$ particles. The capacity retention was also improved when using the surface-modified $LiNi_{0.6}Co_{0.2}Mn_{0.2}O_2$ electrode. The capacity loss of the surface-modified $LiNi_{0.6}Co_{0.2}Mn_{0.2}O_2$ electrode by PEDOT-*co*-PEG was only 6.1% after 100 cycles, while the pristine electrode suffered a 10.7% capacity loss. The good capacity retention in the cell with the surface-modified $LiNi_{0.6}Co_{0.2}Mn_{0.2}O_2$ particles can be ascribed to the presence of a conductive polymer film on the active sites of the cathode. This conductive polymer film functions as a protective layer to cover the active cathode sites and reduce the oxidative decomposition of the electrolyte at high voltage, such that the structural stability of cathode material can be enhanced.

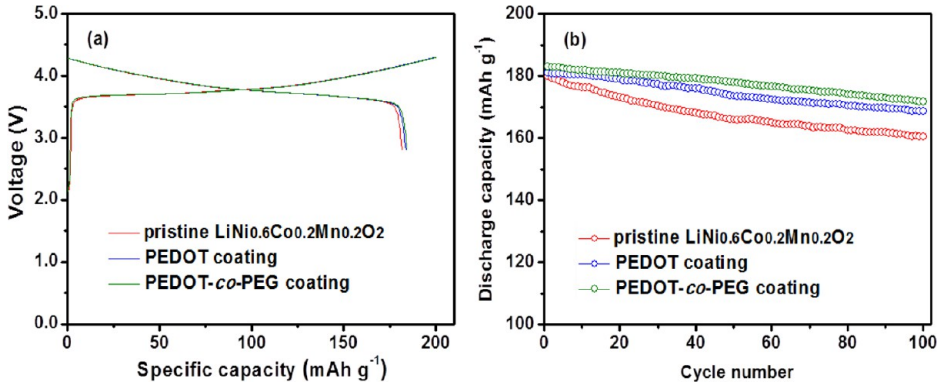

Figure 4. (a) Initial charge and discharge curves of the Li/$LiNi_{0.6}Co_{0.2}Mn_{0.2}O_2$ cells with pristine and surface-modified $LiNi_{0.6}Co_{0.2}Mn_{0.2}O_2$ materials at a constant current rate of 0.1 C between 2.8 and 4.3 V. (b) Discharge capacities of the Li/$LiNi_{0.6}Co_{0.2}Mn_{0.2}O_2$ cells with pristine and surface-modified $LiNi_{0.6}Co_{0.2}Mn_{0.2}O_2$ materials as a function of the cycle number at a constant current rate of 0.5 C.

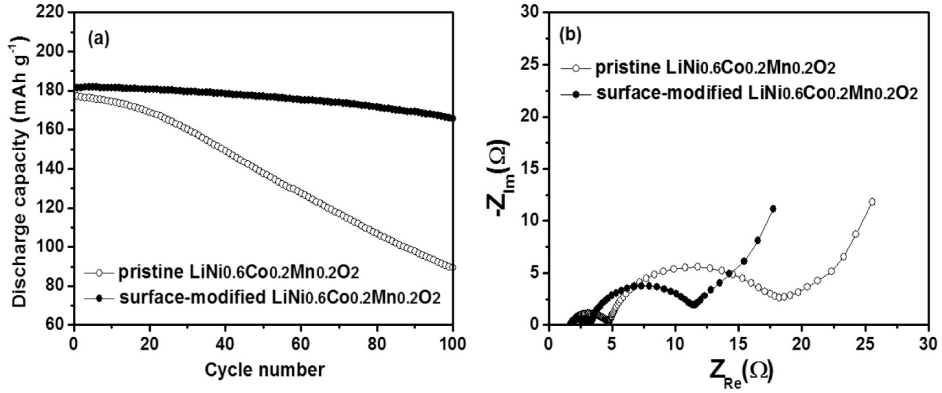

Figure 5. (a) Discharge capacities of the Li/$LiNi_{0.6}Co_{0.2}Mn_{0.2}O_2$ cells with pristine and surface-modified $LiNi_{0.6}Co_{0.2}Mn_{0.2}O_2$ materials at 55 °C and 0.5 C rate as a function of the cycle number. (b) AC impedance spectra of the Li/$LiNi_{0.6}Co_{0.2}Mn_{0.2}O_2$ cells with pristine and surface-modified $LiNi_{0.6}Co_{0.2}Mn_{0.2}O_2$ materials obtained at the charged state after 100 cycles at 55 °C and 0.5 C rate.

Note that the surface-modified $LiNi_{0.6}Co_{0.2}Mn_{0.2}O_2$ electrode using PEDOT-*co*-PEG exhibited a slightly higher initial discharge capacity and better capacity retention than the $LiNi_{0.6}Co_{0.2}Mn_{0.2}O_2$ electrode coated by PEDOT. This result suggests that the surface coating by dual-conductive polymer is more effective for high discharge capacity and good capacity retention. The elasticity of the PEDOT-*co*-PEG polymer layer containing flexible PEG can stabilize the active cathode materials during the volume changes accompanying the charge-discharge processes, resulting in more stable cycling characteristics, as reported by Fedorkova et al.[26,27] Surface morphology of the surface-modified $LiNi_{0.6}Co_{0.2}Mn_{0.2}O_2$ powder after cycling was investigated by TEM analysis, and the results are shown in Figure S4. As can be seen in the figure, the PEDOT-*co*-PEG coating layer is still present on the surface of $LiNi_{0.6}Co_{0.2}Mn_{0.2}O_2$ after 100 cycles, irrespective of charge and discharge state. This result indicates that the charge-discharge processes hardly influence the morphology of the surface layer; therefore, the original particle morphology can be successfully preserved through the cycling for the surface-modified electrode.

Figure 5a shows the discharge capacities of the pristine and surface-modified $LiNi_{0.6}Co_{0.2}Mn_{0.2}O_2$ cathode materials with PEDOT-*co*-PEG, as a function of the cycle number measured at 55 °C and 0.5 C rate. At 55 °C, the pristine and surface-modified $LiNi_{0.6}Co_{0.2}Mn_{0.2}O_2$ cathode materials delivered initial discharge capacities of 180.7 and 184.4 $mAhg^{-1}$, respectively, which are slightly higher than those obtained at 25 °C. The capacity retention was remarkably improved by coating the $LiNi_{0.6}Co_{0.2}Mn_{0.2}O_2$ cathode material with PEDOT-*co*-PEG. It is well known that the gradual capacity fading of layered $LiNi_xCo_yMn_{1-x-y}O_2$ materials at high temperatures is due to structural and interfacial instabilities as well as dissolution of transition metals from the active cathode material by HF attack.[40,41] It is plausible that the protective PEDOT-*co*-PEG layer coated on the active $LiNi_{0.6}Co_{0.2}Mn_{0.2}O_2$ material renders the cathode material more resistive against HF attack in the electrolyte and thus inhibits the dissolution of metals from the active cathode materials into the electrolyte solution at elevated temperatures. As a result, the surface-modified $LiNi_{0.6}Co_{0.2}Mn_{0.2}O_2$ electrode exhibits more stable cycling behavior at 55 °C. In the case of pristine $LiNi_{0.6}Co_{0.2}Mn_{0.2}O_2$, the dissolution of transition metals by HF attack and electrolyte decomposition may cause a rapid increase of the interfacial resistance thereby accelerating the capacity loss as cycling progresses.

In order to understand the effect of the conductive polymer layer on the ac impedance behavior of the Li/$LiNi_{0.6}Co_{0.2}Mn_{0.2}O_2$ cells, ac impedance measurements were performed after cycling at 55 °C. For a fair comparison, the ac impedances of the cells were measured at the charged state of the cell after 100 cycles at 55 °C, and the resultant ac impedance spectra are shown in Figure 5b. In both cells, two overlapping semicircles are observed. According to the previous ac impedance studies,[42,43] the semicircle in the high frequency range can be attributed to the resistance due to Li^+ ion

dx.doi.org/10.1021/am404965p | ACS Appl. Mater. Interfaces 2014, 6, 2546−2552

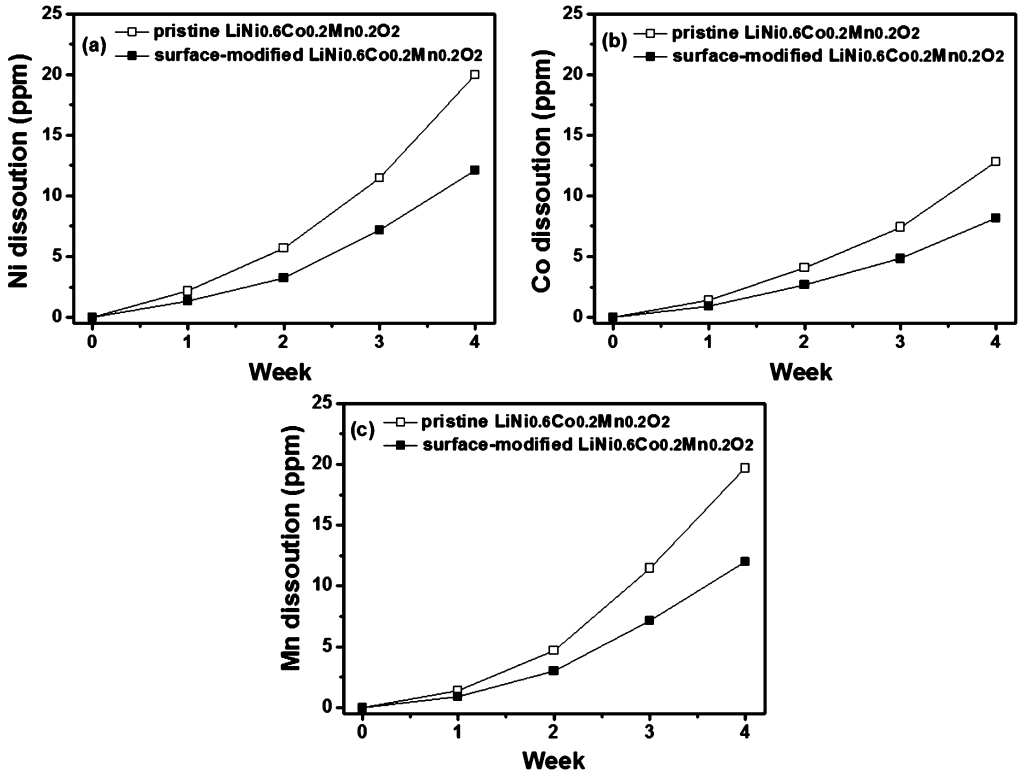

Figure 6. Dissolution of transition metals from the fully charged $LiNi_{0.6}Co_{0.2}Mn_{0.2}O_2$ electrodes into liquid electrolyte as a function of storage time at 55 °C. (a) Ni, (b) Co, and (c) Mn.

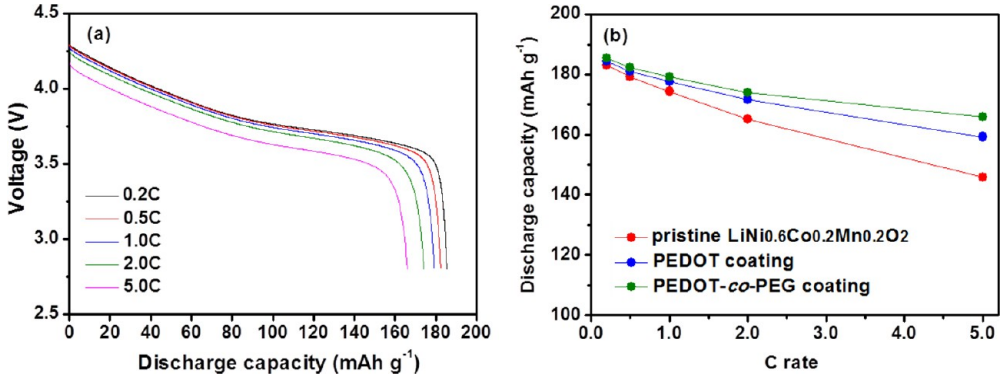

Figure 7. (a) Discharge profiles of the $Li/LiNi_{0.6}Co_{0.2}Mn_{0.2}O_2$ cell with surface-modified $LiNi_{0.6}Co_{0.2}Mn_{0.2}O_2$ by PEDOT-*co*-PEG, as a function of the C rate, and (b) discharge capacities of the $Li/LiNi_{0.6}Co_{0.2}Mn_{0.2}O_2$ cells with pristine and surface-modified $LiNi_{0.6}Co_{0.2}Mn_{0.2}O_2$ materials as a function of the C rate. The charge rate was 0.2 C with a 4.3 V cut-off.

migration through the surface film on the electrode (R_f), while the semicircle observed in the medium-to-low frequency range is due to the charge transfer resistance between the electrode and electrolyte (R_{ct}). Both surface film resistance and charge transfer resistance in the cell with the surface-modified $LiNi_{0.6}Co_{0.2}Mn_{0.2}O_2$ material are lower than those of the cells containing pristine $LiNi_{0.6}Co_{0.2}Mn_{0.2}O_2$. This supports the notion that a protective conductive polymer layer on the cathode limits the growth of a resistive layer due to the oxidative decomposition of electrolyte. A conductive polymer layer on the surface of the active material would also produce good electrical contact between the less conductive $LiNi_{0.6}Co_{0.2}Mn_{0.2}O_2$ particles as well as give rise to protection of the cathode particle from HF attack, which facilitates electron transfer. These results indicate that the surface modification of the $LiNi_{0.6}Co_{0.2}Mn_{0.2}O_2$ active materials by the conductive PEDOT-*co*-PEG layer is very effective for reducing interfacial resistances during cycling at high temperature.

The superior high-temperature cycling stability of the surface-modified $LiNi_{0.6}Co_{0.2}Mn_{0.2}O_2$ electrode with PEDOT-*co*-PEG was further elucidated by measuring the dissolved amount of transition metals at 55 °C. Figure 6 shows that the dissolved amounts of Ni, Co, and Mn are continuously increased with storage time at both pristine and surface-modified $LiNi_{0.6}Co_{0.2}Mn_{0.2}O_2$ electrode. The metal dissolution is due to the attack by HF that is generated as the hydrolysis product of $LiPF_6$ by a small amount of water in the liquid electrolyte, which is mainly responsible for the capacity decline at high temperature.[44−46] The pristine $LiNi_{0.6}Co_{0.2}Mn_{0.2}O_2$ electrode showed higher dissolution of Ni, Co, and Mn after 4 weeks, whereas less amounts of Ni, Co, and Mn are dissolved

from the surface-modified $LiNi_{0.6}Co_{0.2}Mn_{0.2}O_2$ electrode. Thus, it is demonstrated that the PEDOT-*co*-PEG layer is effective in protecting the electrode surface from the attack of HF, contributing to the retardation of metal dissolution. As a result, the $Li/LiNi_{0.6}Co_{0.2}Mn_{0.2}O_2$ cells with surface-modified $LiNi_{0.6}Co_{0.2}Mn_{0.2}O_2$ electrode exhibited better cycling stability at elevated temperature. The cycling stability of surface-modified $LiNi_{0.6}Co_{0.2}Mn_{0.2}O_2$ electrode at elevated temperature was fairly good, considering the transition metals in the surface-modified electrode dissolved quite a bit into the electrolyte. It should be noted that the amount of electrolyte used in the experiment (Figure 6) was quite high, as compared to the amount of electrolyte in the $Li/LiNi_{0.6}Co_{0.2}Mn_{0.2}O_2$ cell (Figure 5), which may cause the dissolution of a larger amount of transition metals into the liquid electrolyte. Accordingly, the metal content dissolved into the liquid electrolyte in the cell during cycling is expected to be much lower than data in Figure 6.

We evaluated the rate capability of the pristine and surface-modified $LiNi_{0.6}Co_{0.2}Mn_{0.2}O_2$ cathode materials at ambient temperature. The cells were charged to 4.3 V at a constant current rate of 0.2 C and discharged at different current rates ranging from 0.2 to 5.0 C. Figure 7a shows the discharge curves of the $Li/LiNi_{0.6}Co_{0.2}Mn_{0.2}O_2$ cells with the surface-modified $LiNi_{0.6}Co_{0.2}Mn_{0.2}O_2$ cathode material using PEDOT-*co*-PEG, as a function of the C rate, and Figure 7b compares the discharge capacities of the $Li/LiNi_{0.6}Co_{0.2}Mn_{0.2}O_2$ cells with the pristine and surface-modified $LiNi_{0.6}Co_{0.2}Mn_{0.2}O_2$ cathode materials using PEDOT or PEDOT-*co*-PEG. The surface-modified $LiNi_{0.6}Co_{0.2}Mn_{0.2}O_2$ cathode material using PEDOT-*co*-PEG delivered the highest discharge capacities at high C rates. For example, the surface-modified $LiNi_{0.6}Co_{0.2}Mn_{0.2}O_2$ electrode using PEDOT-*co*-PEG delivered a discharge capacity of 166.0 mAh g^{-1} at 5 C rate, while the discharge capacities of the pristine and PEDOT-coated $LiNi_{0.6}Co_{0.2}Mn_{0.2}O_2$ electrodes were 145.8 and 159.3 mAh g^{-1}, respectively, at the same current rate. By coating a conductive polymer on the surface of the cathode material, the electronic conductivity was improved, which facilitates the charge transfer reaction. The presence of PEG in the coating layer could also enhance the transport of lithium ions, which is a prerequisite for a fast charge transfer reaction. In this way, the PEDOT-*co*-PEG acts as a conducting network that increases the rate of electron and ion exchange in the depth of the electrode. Thus, the enhanced high rate performance of the surface-modified $LiNi_{0.6}Co_{0.2}Mn_{0.2}O_2$ cathode material using PEDOT-*co*-PEG is explained by the good mixed ionic and electronic conduction of the thin PEDOT-*co*-PEG layer formed on the cathode material.

CONCLUSIONS

The $LiNi_{0.6}Co_{0.2}Mn_{0.2}O_2$ cathode materials with high discharge capacity were synthesized and surface-modified by coating with a dual-conductive PEDOT-*co*-PEG copolymer. The surface-modified $LiNi_{0.6}Co_{0.2}Mn_{0.2}O_2$ cathode material delivered a higher initial discharge capacity and exhibited more stable cycling characteristics than the pristine $LiNi_{0.6}Co_{0.2}Mn_{0.2}O_2$ materials. The presence of the dual-conductive polymer layer formed on the cathode enhanced the high rate performance due to fast ion transport as well as good electrical contact between the $LiNi_{0.6}Co_{0.2}Mn_{0.2}O_2$ particles. It can be concluded that the surface modification of the $LiNi_{0.6}Co_{0.2}Mn_{0.2}O_2$ cathode materials with the dual-conductive PEDOT-*co*-PEG polymer provides a high reversible capacity, stable cycling characteristics, and good rate capability.

ASSOCIATED CONTENT

Supporting Information

Synthetic procedure of $LiNi_{0.6}Co_{0.2}Mn_{0.2}O_2$ materials. SEM image of the pristine $LiNi_{0.6}Co_{0.2}Mn_{0.2}O_2$ powders. FTIR spectra of pristine $LiNi_{0.6}Co_{0.2}Mn_{0.2}O_2$, PEDOT-*co*-PEG, and surface-modified $LiNi_{0.6}Co_{0.2}Mn_{0.2}O_2$. XRD patterns of pristine $LiNi_{0.6}Co_{0.2}Mn_{0.2}O_2$ and surface-modified $LiNi_{0.6}Co_{0.2}Mn_{0.2}O_2$ powders. TEM images of surface-modified $LiNi_{0.6}Co_{0.2}Mn_{0.2}O_2$ powder after repeated cycling. This material is available free of charge via the Internet at http://pubs.acs.org.

AUTHOR INFORMATION

Corresponding Author

*E-mail: dongwonkim@hanyang.ac.kr.

Notes

The authors declare no competing financial interest.

ACKNOWLEDGMENTS

This work was supported by Hyundai Motor Company. This work was also supported by a grant from the Fundamental R&D Program for Core Technology of Materials and a Human Resources Development Program (No. 20124010203290) of KETEP grant funded by the Korean government Ministry of Trade, Industry and Energy.

REFERENCES

(1) Etacheri, V.; Marom, R.; Elazari, R.; Salitra, G.; Aurbach, D. *Energy Environ. Sci.* **2011**, *4*, 3243−3262.
(2) Yang, Z.; Zhang, J.; Kintner-Meyer, M. C. W.; Lu, X.; Choi, D.; Lemmon, J. P.; Liu, J. *Chem. Rev.* **2011**, *111*, 3577−3613.
(3) Venkatraman, S.; Choi, J.; Manthiram, A. *Electrochem. Commun.* **2004**, *6*, 832−837.
(4) Yabuuchi, N.; Ohzuku, T. *J. Power Sources* **2005**, *146*, 636−639.
(5) Liao, P. Y.; Duh, J. G.; Sheen, S. R. *J. Electrochem. Soc.* **2005**, *152*, A1695−A1700.
(6) Santhanam, R.; Rambabu, B. *J. Power Sources* **2010**, *195*, 4313−4317.
(7) Sun, Y. K.; Kim, D. H.; Jung, H. G.; Myung, S. T.; Amine, K. *Electrochim. Acta* **2010**, *55*, 8621−8627.
(8) Luo, W.; Zhou, F.; Zhao, X.; Lu, Z.; Li, X.; Dahn, J. R. *Chem. Mater.* **2010**, *22*, 1164−1172.
(9) Venkateswara Rao, C.; Leela Mohana Reddy, A.; Ishikawa, Y.; Ajayan, P. M. *ACS Appl. Mater. Interfaces* **2011**, *3*, 2966−2972.
(10) Li, Z.; Chernova, N. A.; Roppolo, M.; Upreti, S.; Petersburg, C.; Alamgir, F. M.; Whittingham, M. S. *J. Electrochem. Soc.* **2011**, *158*, A516−A522.
(11) Min, J. W.; Yim, C. J.; Im, W. B. *ACS Appl. Mater. Interfaces* **2013**, *5*, 7765−7769.
(12) Cho, J.; Kim, Y.; Kim, Y.; Park, B. *Angew. Chem., Int. Ed.* **2001**, *40*, 3367−3369.
(13) Gnanaraj, J. S.; Pol, V. G.; Gedanken, A.; Aurbach, D. *Electrochem. Commun.* **2003**, *5*, 940−945.
(14) Chen, Z.; Qin, Y.; Amine, K.; Sun, Y. K. *J. Mater. Chem.* **2010**, *20*, 7606−7612.
(15) Fan, Y.; Wang, J.; Tang, Z.; He, W.; Zhang, J. *Electrochim. Acta* **2007**, *52*, 3870−3875.
(16) Woo, S. U.; Yoon, C. S.; Amine, K.; Belharouak, I.; Sun, Y. K. *J. Electrochem. Soc.* **2007**, *154*, A1005−A1009.
(17) Myung, S. T.; Amine, K.; Sun, Y. K. *J. Mater. Chem.* **2010**, *20*, 7074−7095.
(18) Sclar, H.; Haik, O.; Menachem, T.; Grinblat, J.; Leifer, N.; Meitav, A.; Luski, S.; Aurbach, D. *J. Electrochem. Soc.* **2012**, *159*, A228−A237.

(19) Arbizzani, C.; Mastragostino, M.; Rossi, M. *Electrochem. Commun.* **2002**, *4*, 545−549.
(20) Arbizzani, C.; Balducci, A.; Mastragostino, M.; Rossi, M.; Soavi, F. *J. Power Sources* **2003**, *119-121*, 695−700.
(21) Wang, G. X.; Yang, L.; Chen, Y.; Wang, J. Z.; Bewlay, S.; Liu, H. K. *Electrochim. Acta* **2005**, *50*, 4649−4654.
(22) Huang, Y.-H.; Park, K.-S.; Goodenough, J. B. *J. Electrochem. Soc.* **2006**, *153*, A2282−A2286.
(23) Her, L.-J.; Hong, J.-L.; Chang, C.-C. *J. Power Sources* **2006**, *157*, 457−463.
(24) Park, K.-S.; Schougaard, S. B.; Goodenough, J. B. *Adv. Mater.* **2007**, *19*, 848−851.
(25) Lee, K. S.; Sun, Y. K.; Noh, J.; Song, K.S.; Kim, D. W. *Electrochem. Commun.* **2009**, *11*, 1900−1903.
(26) Fedorkova, A.; Orinakova, R.; Orinak, A.; Talian, I.; Heile, A.; Wiemhofer, H. D.; Kaniansky, D.; Arlinghaus, H. F. *J. Power Sources* **2010**, *195*, 3907−3912.
(27) Fedorkova, A.; Orinakova, R.; Orinak, A.; Wiemhofer, H. D.; Kaniansky, D.; Winter, M. *J. Solid State Electrochem.* **2010**, *14*, 2173−2178.
(28) Sinha, N. N.; Munichandraiah, N. *ACS Appl. Mater. Interfaces* **2009**, *1*, 1241−1249.
(29) Lepage, D.; Michot, C.; Liang, G.; Gauthier, M.; Schougaard, S. B. *Angew. Chem., Int. Ed.* **2011**, *50*, 6884−6887.
(30) Zhan, L.; Song, Z.; Zhang, J.; Tang, J.; Zhan, H.; Zhou, Y.; Zhan, C. *Electrochim. Acta* **2008**, *53*, 8319−8323.
(31) Lee, Y. S.; Lee, K. S.; Sun, Y. K.; Lee, Y. M.; Kim, D. W. *J. Power Sources* **2011**, *196*, 6997−7001.
(32) Yao, Y.; Liu, N.; McDowell, M. T.; Pasta, M.; Cui, Y. *Energy Environ. Sci.* **2012**, *5*, 7927−7930.
(33) Zhou, J.; Lubineau, G. *ACS Appl. Mater. Interfaces* **2013**, *5*, 6189−6200.
(34) Dziewonski, P. M.; Grzeszczuk, M. *Electrochim. Acta* **2010**, *55*, 3336−3347.
(35) Yang, Y.; Yu, G.; Cha, J. J.; Wu, H.; Vosgueritchian, M.; Yao, Y.; Bao, Z.; Cui, Y. *ACS Nano* **2011**, *5*, 9187−9193.
(36) Kang, I. S.; Lee, Y. S.; Kim, D. W. *J. Electrochem. Soc.* **2014**, *161*, A53−A57.
(37) Liu, X.; Li, H.; Li, D.; Ishida, M.; Zhou, H. *J. Power Sources* **2013**, *243*, 374−380.
(38) Wang, Z.; Sun, Y.; Chen, L.; Huang, X. *J. Electrochem. Soc.* **2004**, *151*, A914−A921.
(39) Tang, Z.; Wang, J.; Chen, Q.; He, W.; Shen, C.; Mao, X.-X.; Zhang, J. *Electrochim. Acta* **2007**, *52*, 6638−6643.
(40) Amatucci, G. G.; Tarascon, J. M.; Klein, L. C. *Solid State Ionics* **1996**, *83*, 167−173.
(41) Woo, S. U.; Park, B. C.; Yoon, C. S.; Myung, S. T.; Prakash, J.; Sun, Y. K. *J. Electrochem. Soc.* **2007**, *154*, A649−A655.
(42) Funabiki, A.; Inaba, M.; Ogumi, Z. *J. Power Sources* **1997**, *68*, 227−231.
(43) Levi, M. D.; Salitra, G.; Markovsky, B.; Teller, H.; Aurbach, D.; Heider, U.; Heider, L. *J. Electrochem. Soc.* **1999**, *146*, 1279−1289.
(44) Sun, Y. K.; Hong, K. J.; Prakash, J.; Amine, K. *Electrochem.Commun.* **2002**, *4*, 344−348.
(45) Tasaki, K.; Goldberg, A.; Lian, J. J.; Walker, M.; Timmons, A.; Harris, S. J. *J. Electrochem. Soc.* **2009**, *156*, A1019−A1027.
(46) Liu, J.; Manthiram, A. J. *Phys. Chem. C* **2009**, *113*, 15073−15079.